Journal of Magnetic Resonance 202 (2010) 24–33

Contents lists available at ScienceDirect

Journal of Magnetic Resonance

journal homepage: www.elsevier.com/locate/jmr

Quantitative two-dimensional HSQC experiment for high magnetic field NMR spectrometers

Harri Koskela [a,*], Outi Heikkilä [b], Ilkka Kilpeläinen [c], Sami Heikkinen [c]

[a] VERIFIN, University of Helsinki, P.O. Box 55, FIN-00014 Helsinki, Finland
[b] Folkhälsan Institute of Genetics, Folkhälsan Research Center, Biomedicum Helsinki, University of Helsinki, P.O. Box 63, FIN-00014, Finland
[c] Laboratory of Organic Chemistry, University of Helsinki, P.O. Box 55, FIN-00014 Helsinki, Finland

ARTICLE INFO

Article history:
Received 24 June 2009
Revised 11 September 2009
Available online 30 September 2009

Keywords:
Quantitative two-dimensional NMR
^{13}C offset compensation
Carr–Purcell–Meiboom–Gill sequences
Adiabatic inversion pulses
PM-BEBOP
Q-OCCAHSQC
Human blood plasma

ABSTRACT

The finite RF power available on carbon channel in proton–carbon correlation experiments leads to non-uniform cross peak intensity response across carbon chemical shift range. Several classes of broadband pulses are available that alleviate this problem. Adiabatic pulses provide an excellent magnetization inversion over a large bandwidth, and very recently, novel phase-modulated pulses have been proposed that perform 90° and 180° magnetization rotations with good offset tolerance. Here, we present a study how these broadband pulses (adiabatic and phase-modulated) can improve quantitative application of the heteronuclear single quantum coherence (HSQC) experiment on high magnetic field strength NMR spectrometers. Theoretical and experimental examinations of the quantitative, offset-compensated, CPMG-adjusted HSQC (Q-OCCAHSQC) experiment are presented. The proposed experiment offers a formidable improvement to the offset performance; ^{13}C offset-dependent standard deviation of the peak intensity was below 6% in range of ±20 kHz. This covers the carbon chemical shift range of 150 ppm, which contains the protonated carbons excluding the aldehydes, for 22.3 T NMR magnets. A demonstration of the quantitative analysis of a fasting blood plasma sample obtained from a healthy volunteer is given.

1. Introduction

Nuclear magnetic resonance (NMR) spectroscopy is one of the most important analytical techniques in chemistry for characterization of molecular structures. In addition to the detailed structural information, NMR spectroscopy gives accurate quantitative information about the sample constituent, and therefore quantitative ^{1}H NMR has become an important tool in analysis of natural products and in metabolomics [1,2]. The interest to study mixtures of increasing complexity has create the demand to employ high magnetic field NMR spectrometers to improve resolution and sensitivity. However, quantification of complex samples with ^{1}H NMR spectroscopy suffers from resonance overlap even at high magnetic fields, which can prevent accurate quantification of sample compounds. Proton–carbon correlated two-dimensional (2D) NMR experiments exploit the wide chemical shift range of carbon, thus offering a significantly improved resolution. Therefore, the application of proton–carbon correlated 2D NMR experiments in determination of molar concentration of the sample compounds has gained interest in studies of natural products, biological samples and processes taking place in living organisms [3].

While many of the quantitative studies presented in literature are performed using a standard heteronuclear single quantum coherence (HSQC) experiment, several modifications of the basic pulse sequence have been proposed in recent years to improve the quantitativity of the data. Previously, an experiment called as Q-HSQC [4], was presented, where the $^1J_{CH}$-dependence of correlation peak volumes was compensated by selecting four polarization transfer values for the constant-time INEPT (Insensitive Nuclei Enhanced by Polarization Transfer) [5] periods. The sum of these acquisitions was recorded for each increment in order to produce uniform intensity response over the $^1J_{CH}$ coupling range of 115–220 Hz. The relatively long constant-time INEPT periods in the Q-HSQC experiment led to distorted lineshapes, especially when a proton had several J_{HH} couplings, thus causing problems in the cross peak integration. This problem was addressed later in the Q-CAHSQC experiment [6] where the influence of the J_{HH} coupling evolution was avoided with use of Carr–Purcell–Meiboom–Gill (CPMG) [7,8] pulse trains by replacing the constant-time INEPT periods with the constant-time CPMG-INEPT steps. Recently, an interesting modification of the Q-CAHSQC experiment, QQ-HSQC, was proposed by Peterson and Loening [9]. Their experiment elegantly exploited spatial encoding of the sample volume [10–12] in a way that the different parts of the sample were optimized for different polarization transfer evolutions, resulting in reduced

* Corresponding author. Fax: +358 9 191 50437.
E-mail address: Harri.T.Koskela@helsinki.fi (H. Koskela).

1090-7807/$ - see front matter © 2009 Elsevier Inc. All rights reserved.
doi:10.1016/j.jmr.2009.09.021

number of scans per increment and therefore shorter total acquisition time with concentrated samples.

The wide chemical shift range of the carbon dimension can compromise quantitativity of these experiments; the finite RF power available is insufficient for uniform excitation of the whole carbon chemical shift range with normal rectangular pulses. Obviously, this problem becomes more pronounced with increasing magnetic field strength. Typical NMR spectrometer RF amplifiers deliver high-power RF strength of 20 kHz on carbon channel. This RF strength gives a reasonably uniform excitation with standard rectangular RF pulses for the 200 ppm carbon chemical shift range at 9.4 T magnetic field strength ($\nu(^{13}C)$ = 100.6 MHz, 200 ppm ≈20 kHz). If the magnetic field strength is doubled (18.8 T, $\nu(^{13}C)$ = 201.2 MHz) the 200 ppm carbon chemical shift range corresponds to ca. 40 kHz, making the 20 kHz RF strength insufficient for uniform excitation with standard rectangular pulses. Therefore, a good offset performance of ^{13}C channel RF pulses is essential for quantification purposes.

There are several options to improve the performance of the RF pulses with finite amplitude. A traditional approach is to use composite pulses [13,14], that are designed to fulfill either inversion [15–17], refocusing [18–20], excitation [21,22], or even arbitrary nutation [23] of the magnetization. Another technique specifically designed for uniform manipulation of magnetization over a wide chemical shift range utilizes adiabatic fast passages [24,25]. The broadband pulses have been successfully applied to compensate the off-resonance effects in 2D ^{1}H–^{13}C correlation experiments [26–29] and 2D ^{1}H–^{15}N correlation experiments [30], but their application in quantitative 2D NMR needs some consideration. The main focus in our study was to find suitable ^{13}C pulse elements for HSQC-type experiments in order to develop a quantitative 2D proton-carbon correlation experiment usable in high magnetic field strengths.

2. Experimental

2.1. Materials

Offset profile tests were performed with a test sample containing 10% MeOH in MeOH-*d*4 in a 5 mm NMR tube (Bruker BioSpin, Germany). Strychnine sample was prepared by dissolving 39 mg of strychnine (Sigma–Aldrich) in 0.8 ml $CDCl_3$ (Sigma–Aldrich). This solution was transferred to 5 mm NMR tube (Wilmad 507-PP). The fasting blood plasma sample was obtained from a healthy volunteer. The amount of 550 μL of blood plasma and 60 μL of D_2O (to provide deuterium lock) were transferred into 5 mm NMR tube (Wilmad 507-PP) for NMR measurements.

2.2. Simulations

Density matrix calculations were performed using GAMMA toolkit [31] on MS Visual C++ 6.0. The produced data was plotted using MATLAB [32].

2.3. NMR experiments

The NMR experiments were carried out at 11.75 T ($\nu(^{1}H)$ = 500 MHz, $\nu(^{13}C)$ = 125.8 MHz) using a Bruker DRX 500 NMR spectrometer equipped with a 5 mm inverse *z*-gradient broadband probe head (Bruker BioSpin, Germany).

The Q-OCCAHSQC experiment (Fig. 1) employed adiabatic tanh/tan inversion pulses [33] on carbon channel in the XY-16 pulse trains [34] in the constant-time CPMG-INEPT periods (sections I and III). The PM-BEBOP pulses [35] in the section II were used for 90° and 180° rotations. Adiabatic decoupling was performed with CHIRP-95 pulses [36].

The strychnine sample was measured at 290 K using two scans per Δ-value, resulting in total of eight scans per increment. The number of dummy scans was 32. Spectral widths in the proton and carbon dimensions were 10 ppm and 200 ppm, respectively. The carrier frequencies for proton and carbon were 5.0 ppm and 100 ppm (if not stated otherwise). The repetition time was set to 15.8 s which equals to five times the longest T_{1H} of the sample (H-4). The 2D spectrum was acquired with 4k * 400 points. Total measurement time was 15 h: 57 min.

The 1D Q-OCCAHSQC spectra were integrated with TopSpin. The resonance intensities in 1D CPMG spectrum of blood plasma were determined with PERCH 2008/1-software (PERCH Solutions Ltd., Kuopio, Finland) using constrained total-lineshape-fitting deconvolution [37]. The same software was used to determine J_{HH} couplings from ^{1}H NMR spectrum of strychnine. The 2D spectra were integrated using XwinNMR 3.0 (Bruker BioSpin, Germany) by direct summation of the spectral data points in the cross peaks.

3. Results and discussion

The strategy in development of a quantitative 2D proton-carbon correlation experiment usable in high magnetic field strengths was to start with the basic construct of Q-CAHSQC [6], as this pulse sequence is designed for uniform intensity response over a large range of $^{1}J_{CH}$ couplings and for suppression of J_{HH} coupling evolution distortions during the constant-time CMPG-INEPT periods (Fig. 1). The ^{13}C offset performance of suitable pulse elements was analyzed with theoretical simulations and verified with experimental tests. Quantitativity of the experiment was evaluated using a model chemical (strychnine) and an analysis of a real mixture sample (human blood plasma) was demonstrated.

3.1. Simulations

Various mathematical methods can be used to describe the behavior of magnetization in NMR. The Bloch equations [38] effectively present the evolution of bulk magnetization, but they have only limited ability to describe evolution of *J* couplings as well as multiple-quantum coherences. Product operator formalism [39] provides tools to follow multiple-quantum coherence evolution by simple transformations of spin operators, but it is not suitable to analyze offset effects in detail. A thorough and rigorous analysis of spin dynamics is, however, possible with density matrix calculations [40]. Therefore, this approach was applied in the simulations.

First task was to investigate the ^{13}C offset and B_1 inhomogeneity tolerance of the polarization transfer steps of the pulse sequence (Fig. 1, sections I and III). The earlier Bloch simulations suggested that XY-16 pulse train itself has a good offset compensation even with rectangular pulses [6]. A more realistic model of the actual polarization transfer with respect to ^{13}C offset and B_1 inhomogeneity was examined with density matrix calculations for the AX spin system (A = ^{1}H, X = ^{13}C) with J_{AX} = 140 Hz. For simulation purposes, $\gamma B_1^0 (\gamma = \gamma/2\pi)$ was set to 20 kHz, the spoiler gradient pulses, gradient coherence selection and t_1 evolution period were omitted, ideal proton pulses were used, and the carbon pulses within pulse sequence section II were applied on-resonance with ideal RF strength (Fig. 1). The results indicated that the compensation of B_1 inhomogeneity effects was excellent and ^{13}C offset performance was relatively good with normal rectangular 180° pulses in the CPMG-INEPT periods (Fig. 2A); the bandwidth where 95% transfer efficiency was achieved was ca. ±6.5 kHz with $B_1/B_1{}^0$ = 1. This ^{13}C offset performance is, however, not sufficient when operating with high magnetic field spectrometers with field strengths above 14.1

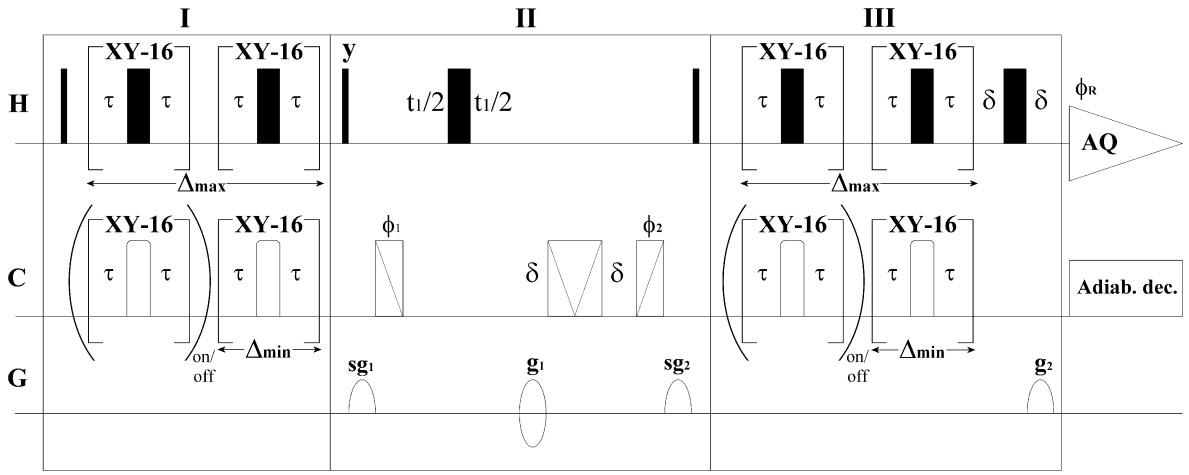

Fig. 1. Pulse sequence for the Q-OCCAHSQC experiment. Narrow and wide filled rectangles represent the rectangular 90° and 180° pulses, respectively. The rounded open rectangles represent broadband inversion pulses (tanh/tan, pulse width 122 μs, R = 110, Q = 5, number of points = 244), and the open rectangles with diagonal lines in the section II represent broadband PM-BEBOP [35] pulses for $M_z \rightarrow M_x$ rotation, universal 180° rotation, and $M_x \rightarrow M_z$ rotation with durations of 1 ms, 2 ms, and 1 ms, respectively; γB_1 was 15.0 kHz. Pulse phases are along x axis if not stated otherwise. Phase cycles were $\phi_1 = \{x, -x, x, -x,\}$, $\phi_2 = \{x, x, -x, -x\}$, and $\phi_R = \{x, -x, -x, x\}$. The pulsed field gradients are represented by half-ellipses. The constant-time CPMG-INEPT periods (sections I and III) consist of the XY-16 pulse trains [34] with total duration of Δ_{max}. Each of XY-16 pulse trains consist of 16 centered 180° pulses on both channels with phases $\{x, y, x, y, y, x, y, x, -x, -y, -x, -y, -y, -x, -y, -x\}$, and 32 τ-delays. The delay τ in the CPMG-INEPT periods must be short enough to satisfy the condition $\tau < 1/(2 * \Delta\nu_{max})$, where $\Delta\nu_{max}$ is the maximum chemical shift difference (in Hz) of coupled protons. In order to give the uniform intensity response over the wide range of $^1J_{CH}$ values, four acquisitions with different polarization transfer times (of which three transfer times were equal) for the constant-time CPMG-INEPT periods (Δ_{min}, Δ_{min}, Δ_{min}, Δ_{max}) were recorded for each increment (for both echo and antiecho part). This was accomplished by setting the second XY-16 pulse train duration in the constant-time CPMG-INEPT period (sections I and III) to Δ_{min}., and switching the carbon channel pulsing of the first XY-16 pulse train either on or off in the following order: (off, off, off, on). In the earlier paper [4] these polarization transfer times were iteratively optimized for the $^1J_{CH}$-range of 115–190 Hz, and the best values were Δ_{min} = 2.94 ms and Δ_{max} = 5.92 ms. New Δ_{min} and Δ_{max} values (3.72 ms and 7.45 ms, respectively) were iteratively calculated for this study (see Section 3). The PFG duration was 1 ms, with eddy-current recovery delay of 100 μs, giving the delay Δ a duration of 1.1 ms. The applied PFG strengths were g_1 = 48 G/cm and g_2 = 12 G/cm, and the corresponding spoiler PFG strengths were sg_1 = 54 G/cm and sg_2 = 44 G/cm. For every increment of t_1, minimum of two-step phase cycle was conducted per every polarization transfer value, and the same was done with changed polarity of g_1 for the gradient-based echo-anti-echo quadrature detection in the F_1-dimension. The axial peak displacement was achieved with the States-TPPI method by inverting the phases ϕ_1 and ϕ_R on every second increment of t_1. The asynchronous adiabatic decoupling was accomplished with CHIRP-95 pulses [36] (pulse width 1.5 ms, R = 90, Q = 5, number of points = 1000) using M4P5 supercycle [63] on ^{13}C channel during acquisition.

T ($\nu(^{13}C)$ = 150.9 MHz), as the ^{13}C chemical shift range of 150 ppm exceeds 22 kHz. Kövér and co-workers [41] applied composite 180° pulses, $90°_{(x)}$–$180°_{(y)}$–$90°_{(x)}$ [15], in the CPMG-INEPT period of their CPMG-HSQMBC experiment in order to improve the ^{13}C inversion bandwidth. Density matrix calculations indicated, that the tolerance of ^{13}C offset as well as B_1 inhomogeneity was considerably better when the rectangular 180° pulses were replaced with composite 180° pulses (Fig. 2B). It was also evident that the composite 180° pulse-based CPMG-INEPT polarization transfer profile was not smooth but instead contained variation in the intensity, which will compromise the quantitativity. Adiabatic pulses are considered to be excellent when uniform broadband inversion is needed, but the pulse durations are typically long, ranging from several hundred microseconds to several milliseconds. The delay τ in the CPMG-INEPT periods must be short enough to satisfy the condition $\tau < 1/(2 * \Delta\nu_{max})$, where $\Delta\nu_{max}$ is the maximum encountered chemical shift difference of coupled protons in hertz, for proper J_{HH} evolution suppression [42–47]. If long adiabatic ^{13}C pulses are applied in the CPMG-INEPT step simultaneously with much shorter proton 180° pulses, the proton interpulse delay can exceed the aforementioned condition. Hwang and co-workers [33] have earlier presented adiabatic tanh/tan pulses, which offer excellent broadband inversion capabilities with relatively short pulse durations. For our purposes, the tanh/tan pulse duration was slightly reduced (122 μs) from the previously presented optimal duration (192 μs) [33] in order to get a compromise between the inversion bandwidth and the J_{HH} suppression condition. The density matrix calculations showed an excellent polarization transfer properties over a wide range of ^{13}C offset and B_1 inhomogeneity (Fig. 2C). Therefore tanh/tan pulses were selected to replace ^{13}C inversion pulses in the constant-time CPMG-INEPT periods.

The second task was to simulate magnetization rotation properties of the ^{13}C pulses presented in section II of the pulse sequence (Fig. 1). For simulation purposes, the spoiler gradient pulses, gradient coherence selection and t_1 evolution period were omitted, and only ^{13}C pulses were considered. If rectangular 90° and 180° pulses are used, the tolerance of ^{13}C offset and B_1 inhomogeneity is limited (Fig. 2D). In the previous paper [6] a partial solution to this problem was proposed by applying specific 90° composite pulses for $M_z \rightarrow -M_y$ and $-M_y \rightarrow -M_z$ rotations. The Bloch simulations [6] suggested reasonably uniform rotation performance over bandwidth of $\pm 0.3 * (\gamma B_1$, which was also confirmed with density matrix calculations (Fig. 2E), but the performance is not sufficient in higher magnetic field strengths. Recently, Skinner and co-workers [35] have presented a class of RF pulses iterated with optimal control algorithm. These PM-BEBOP pulses (phase-modulated broadband excitation by optimized pulses) have an excellent performance in 90° and 180° magnetization rotations. The ^{13}C pulses shown in section II of the pulse sequence (Fig. 1) were replaced with the PM-BEBOP pulses intended for $M_z \rightarrow M_x$ rotation, universal 180° rotation, and $M_x \rightarrow M_z$ rotation. Based on density matrix calculations (Fig. 2E) the magnetization rotation efficiency for $M_z \rightarrow M_x \rightarrow -M_x \rightarrow M_z$ rotations is practically flawless in the studied range of ^{13}C offset and B_1 inhomogeneity, so the PM-BEBOP pulses were selected to replace ^{13}C pulses in section II of the pulse sequence (Fig. 1).

As the constant-time CPMG-INEPT periods now use relatively long adiabatic inversion pulses, the Δ_{min} and Δ_{max} values presented in the earlier study were not optimal to produce uniform intensity response over the natural range of $^1J_{CH}$ couplings. The polarization transfer efficiency for the AX spin system with a total of 21 evenly spaced J coupling values in range of 115–220 Hz were

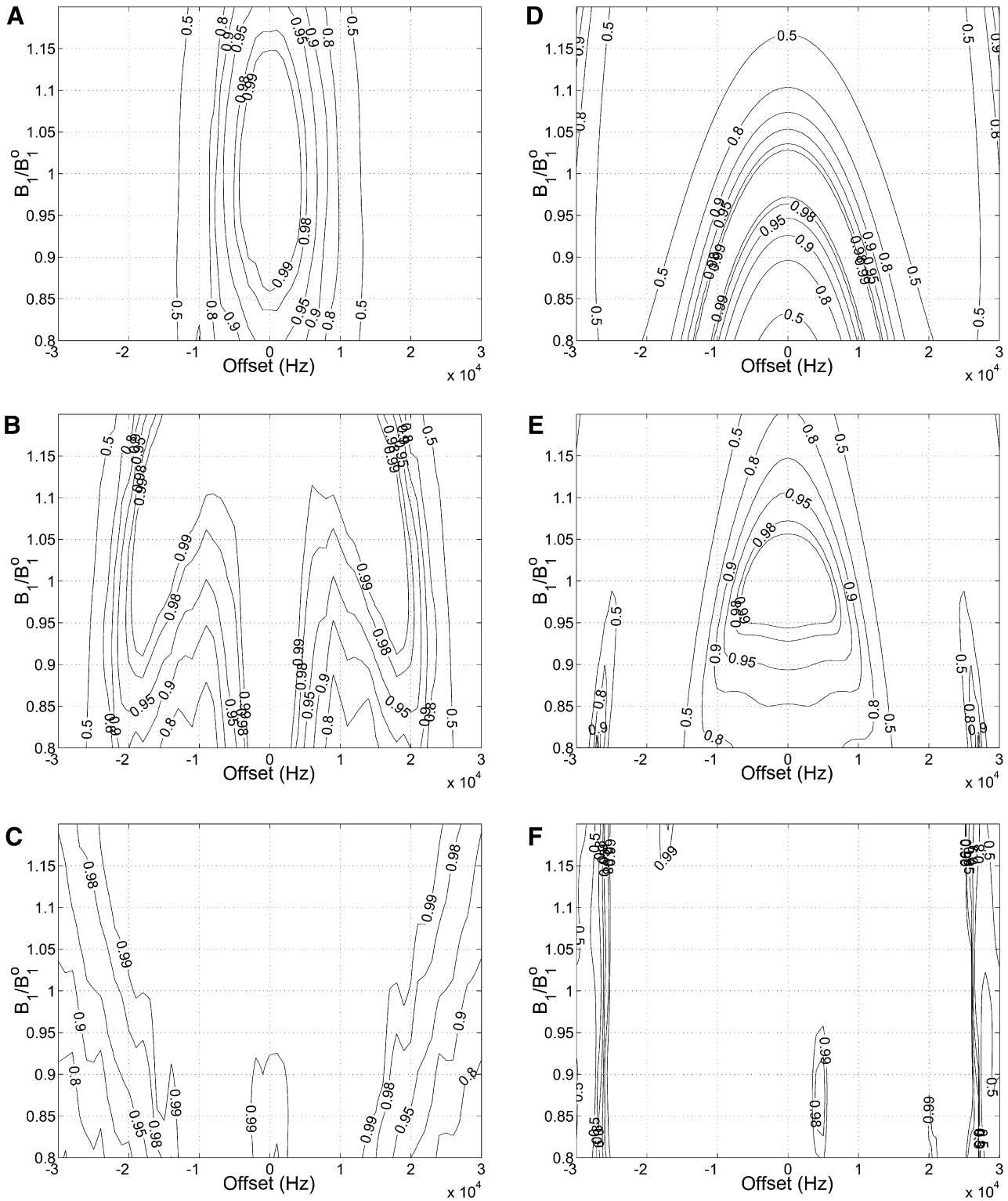

Fig. 2. Simulated polarization transfer and magnetization rotation efficiency profiles for selected pulse sequence parts with respect to the ^{13}C pulse offset and B_1 inhomogeneity. The left pane represents the $H_z \rightarrow H_x$ polarization transfer efficiency for the AX (A = ^1H, X = ^{13}C, J_{AX} = 140 Hz) spin system with respect to ^{13}C pulse performance in constant-time CPMG-INEPT periods (Fig. 1, sections I and III) when carbon pulses are (A) rectangular 180° pulses with $\gamma B_1 = 20$ kHz, (B) composite inversion pulses ($90_{(x)}$–$180_{(y)}$–$90_{(x)}$) [15] with $\gamma {B_1}^0 = 20$ kHz, and (C) adiabatic tanh/tan inversion pulses with $\gamma {B_1}^0{}_{max} = 18.466$ kHz. The right pane represent the $M_z \rightarrow \pm M_z$ rotation efficiencies with respect to ^{13}C pulses in the section II (see Fig. 1) when the needed rotation is (A) $M_z \rightarrow -M_y \rightarrow M_y \rightarrow M_z$ using rectangular 90° and 180° pulses with $\gamma {B_1}^0 = 20$ kHz, (B) $M_z \rightarrow -M_y \rightarrow -M_z$ using composite 90° pulses ($360_{(x)}$–$270_{(-x)}$–Δ' [22] and $385_{(x)}$–$320_{(-x)}$–$25_{(x)}$ [21], $\Delta' = 2 * PW_{90}/\pi$, ($\gamma {B_1}^0 = 20$ kHz) as presented in the previous study [6], and (C) $M_z \rightarrow M_x \rightarrow -M_x \rightarrow M_z$ with PM-BEBOP 90° and 180° rotation pulses ($\gamma {B_1}^0 = 15.0$ kHz) [35]. The transfer/rotation efficiency is presented with contours at levels 0.5, 0.8, 0.9, 0.95, 0.98, and 0.99.

calculated using the earlier Δ_{min} and Δ_{max} values [4,6]; the simulated pulses were kept on-resonance with optimal RF strengths. The standard deviation of the polarization transfer efficiencies for the sampled J coupling values was minimized by iterating Δ_{min}

and Δ_{max} in step-wise fashion. Final result gave Δ_{min} and Δ_{max} values of 3.72 ms and 7.45 ms, respectively, with standard deviation of the efficiencies below 1% in the calculated J coupling range. The uniformity of the J coupling response with respect to the ^{13}C offset was also tested. The result with the AX spin system showed that the normalized polarization transfer efficiency over the J coupling range of 115–220 Hz of the simulated Q-OCCAHSQC experiment was above 95% in offset range of ±15 kHz, and above 90% in offset range of ±20 kHz (Fig. 3).

3.2. Offset profile studies

First, the experimental offset profile of the tanh/tan pulses in the constant-time CPMG-INEPT periods (Fig. 1, sections I and III) was monitored. The test was performed measuring the 1D Q-OCCAHSQC spectra from methanol. The tanh/tan pulse offset was varied in range of ±30 kHz in 1 kHz steps, all other pulses were applied on-resonance. No ^{13}C decoupling was applied during acquisition in order to monitor any lineshape anomalies (phase error, antiphase lineshape distortion) more clearly. The results in Fig. 4A show that the experimental data is in accordance with the simulation results (see Fig. 2C). No significant phase anomalies were observed in the offset range of ±20 kHz. Small intensity attenuation and antiphase lineshape distortions were observed outside this offset range.

The experimental offset profile was also inspected for the PM-BEBOP pulses present in section II of the pulse sequence. As can be seen from Fig. 4B, the experimental intensity and lineshape behavior is not as good as could have been anticipated from the simulation results (see Fig. 2F). The most likely explanation for the experimental results arises from the fact that the PM-BEBOP pulses are constructed from small (1.6 μs) pulse steps with abrupt phase changes. The electronics of the spectrometer must accomplish fast phase changes in range of 0–360° with high accuracy in order to deliver the PM-BEBOP pulses as intended. It was therefore assumed that the performance of the older generation spectrometer at our disposal was not completely up to this task. Adiabatic pulses like tanh/tan, in turn, have smoother phase profile in their shape, so they are easier for the spectrometer hardware. It is possible that the more up-to-date hardware can perform the PM-BEBOP pulses with higher accuracy, giving more uniform results.

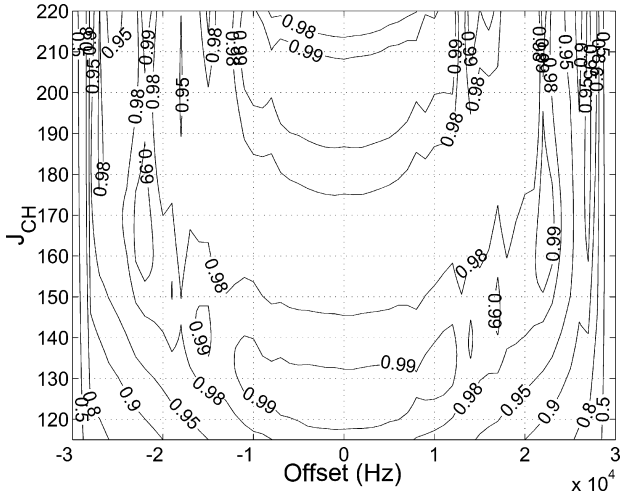

Fig. 3. Simulated normalized polarization transfer efficiency profile of Q-OCCA-HSQC experiment for the AX (A = ^{1}H, X = ^{13}C) spin system with respect to the ^{13}C offset and J_{CH} coupling. The transfer efficiency is presented with contours at levels 0.5, 0.8, 0.9, 0.95, 0.98, and 0.99.

Nevertheless, the lineshape and intensity errors were acceptable considering the good offset performance of the PM-BEBOP pulses.

Next, the performance of adiabatic decoupling sequence utilizing CHIRP-95 pulses was tested. CHIRP-95 pulses have been reported to perform well over broad bandwidths with a good tolerance for variations in the RF amplitude [36]. The adiabatic decoupling was optimized for the studied offset range (±30 kHz). The offset of decoupling sequence was varied while all other pulses were applied on-resonance. Fig. 4C shows that the peak intensity is uniform within the offset range of ±23 kHz. The subharmonic sidebands are more pronounced when the offset increases above ±10 kHz. The decoupling sidebands can be cancelled with various schemes [48–50], but these methods do not restore the original main peak intensity. It is possible, especially when spectrum is crowded, that decoupling sideband appears at the same position with another real cross peak, giving a small contribution to the volume. In those cases it is advisable to apply these sideband cancellation schemes.

The final ^{13}C offset profile test with the 1D Q-OCCAHSQC experiment was performed by changing the ^{13}C carrier frequency (i.e. for all ^{13}C pulses and decoupling) over the studied offset range (±30 kHz). Fig. 4D shows that there are some fluctuations in the peak intensities and phases. Comparison between Fig. 4D and B shows that the main contribution to these fluctuations is arising from PM-BEBOP pulses. Table 1 shows the standard deviations and maximum errors of the peak integrals in specific offset ranges. The peak integrals drop significantly when the offset is over ±23 kHz, and there is a local minimum around −20 kHz offset. In overall, results with acceptable reliability can be achieved (standard deviation under 6%) within the offset range of ±20 kHz. This corresponds to roughly the 150 ppm range at 22.3 T ($\nu(^{13}C)$ = 238.9 MHz) NMR magnets, which covers typically the ^{13}C shift range of aliphatic, aromatic, and olefinic carbons. If also the aldehydes are to be included in the 2D spectrum, then carbon shift range is ca. 200 ppm. This chemical shift range is still covered for 17.6 T ($\nu(^{13}C)$ = 188.6 MHz) NMR magnets.

4. 2D quantification

The 2D quantification tests were performed with a strychnine sample. Strychnine is an ideal test chemical for quantification as it has a complex network of J_{HH} couplings and a large chemical shift range for both proton and carbon resonances. The experiments were performed at 11.75 T ($\nu(^{13}C)$ = 125.8 MHz) NMR magnet field strength. This spectrometer at our disposal is nowadays not regarded as a high field NMR spectrometer, but the loss of cross peak intensity due to offset effects is already well observed at this field strength [6]. In the Q-HSQC and Q-CAHSQC spectra of strychnine [6] the offset effects caused cross peaks with large ^{13}C offset to have over 40% smaller peak integrals compared to cross peaks with small ^{13}C offset. In the Q-OCCAHSQC spectra where the ^{13}C carrier frequency was set in the middle of the carbon chemical shift range, this offset-dependent cross peak volume loss was negligible; the integrals of the cross peaks with the largest carbon offset, 15a and 15b (see Ref. [6] for numbering), are within 5% of the reference integral value (Table 2, the reference cross peak 4 almost on-resonance in ^{13}C channel). The average of integration results was close to the reference cross-peak integral, and standard deviation was relatively small, indicating that the experiment can be applied to distinguish methyl, methylene, and methine cross peaks and the total number of non-exchanging protons on the basis of the cross-peak integrals similarly as with ^{1}H NMR.

In order to test the offset effects on the cross-peak integral values at the extreme offset frequencies determined during the offset profile studies (see above), the ^{13}C carrier frequency for RF pulses

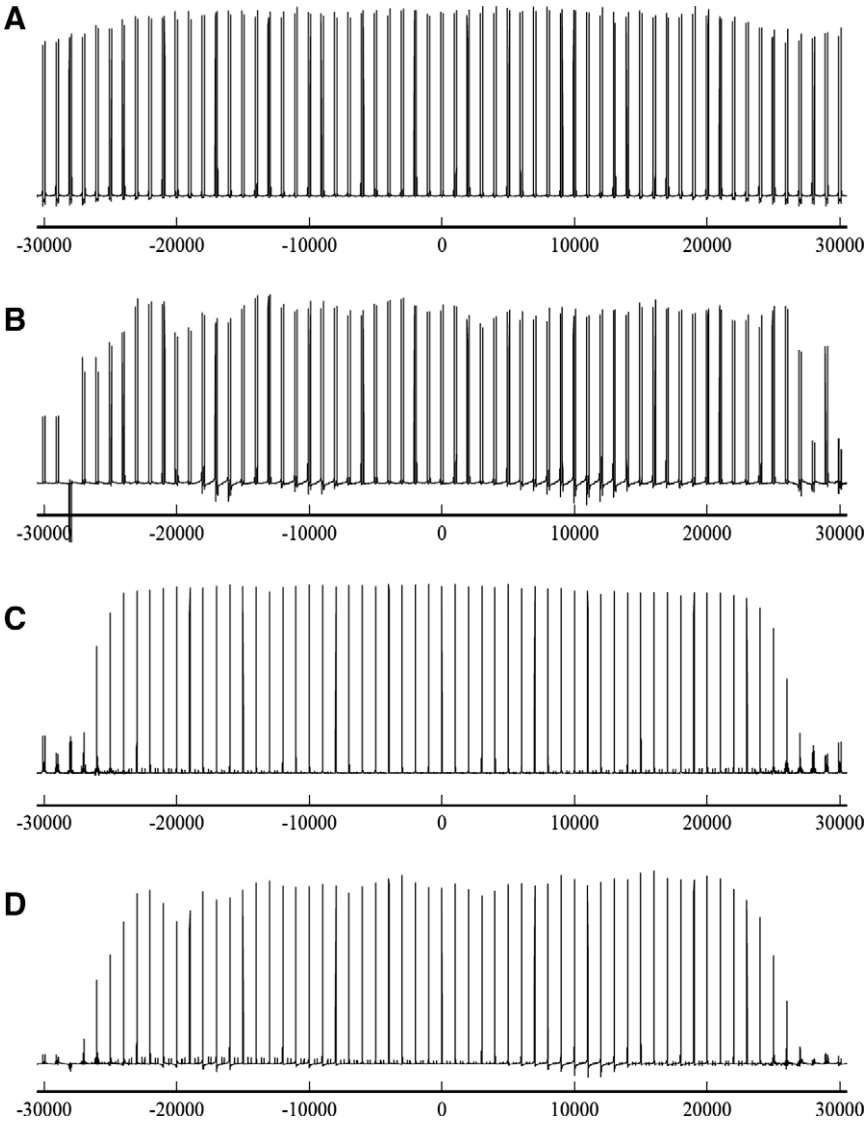

Fig. 4. 1D Q-OCCAHSQC spectrum arrays from methanol sample at 290 K. The measurement of the one-dimensional Q-OCCAHSQC experiment was performed by omitting the t_1 evolution period. The spectrum arrays are measured varying the ^{13}C offset in range of ±30 kHz (1 kHz step) for (A) the CPMG-INEPT periods, (B) the PM-BEBOP pulses, (C) adiabatic decoupling, and (D) the ^{13}C carrier frequency. The spectrum arrays (A) and (B) are measured without adiabatic decoupling in order to observe possible lineshape anomalies (phase errors, antiphase lineshape distortions). Spectral width in the proton dimension was 1.68 ppm. The on-resonance carrier frequencies for proton and carbon were 3.37 ppm and 48.84 ppm, respectively. Two scans were acquired per Δ-value, resulting in total of eight scans. The number of dummy scans was four. The 1D spectrum was acquired with 1k points. The repetition time was set to 10 s. Line broadening (LB) of 1 Hz was used in apodization. The number of real points after Fourier transforms was 2 k.

and adiabatic decoupling was set to 200 ppm. In this way the carbon offset of the 15a, 15b cross peaks would be ca. −21.8 kHz, which is slightly over the recommended bandwidth of ±20 kHz. The results in Table 2 indicate that these cross peaks with the largest ^{13}C offset have attenuated ca. 20% from the reference value, suggesting that C-15 does not experience optimal RF pulses anymore. On the other hand, the cross peaks of 11a and 11b, which are inside the recommended ^{13}C offset range, deviate only 4% from the reference integral value. It should be noted, that there are some cross peaks within the optimal offset range that have relatively large deviations from the reference integral value. In both experiments the cross peak of 18b has the highest deviation, suggesting that there is a ^{13}C offset-independent factor involved. The proton 18b has very large J_{HH} couplings with geminal and vicinal protons ($^2J_{H18b,H18a} = -10.2$ Hz, $^3J_{H18b,H17a} = 4.0$ Hz, $^3J_{H18b,H17b} = 14.6$ Hz). As discussed in the earlier paper [6], Hartmann-Hahn transfer between protons during the constant-time CPMG-INEPT periods can cause attenuation of the cross peak intensities. This attenuation must be realized when using single cross peaks as the basis of quantification in mixture samples, as it may give a systematic error in the quantification results. It is therefore recommended in mixture sample analyses to integrate all viable cross peaks from the quantified compound, and use their average to represent the quantity. If this is not possible or desired, the cross peaks that are used for quantification should preferably be narrow and intense with only a few J_{HH} couplings, e.g. methyl cross peaks.

4.1. Plasma sample analysis

Quantitative ^1H NMR is an important tool in investigation of metabolic diseases from human blood plasma and serum [51,52]. While experimentally the ^1H NMR analysis of plasma samples is quite straightforward, the interpretation and extraction of quantitative information is difficult due to large distribution of both low and high molecular weight components present in the plasma. The ^1H NMR spectra can be simplified using relaxation or diffusion-

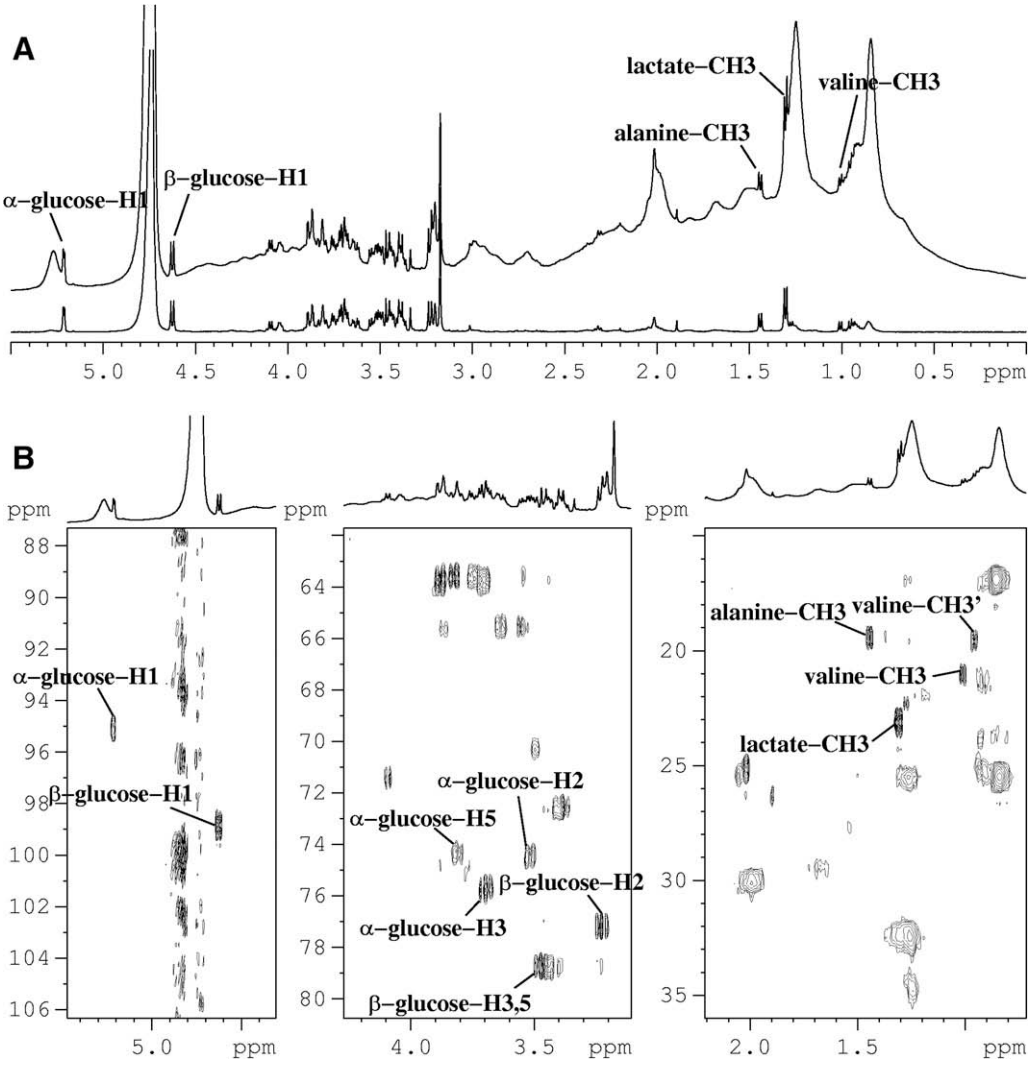

Fig. 5. NMR spectra from human blood plasma sample at 300 K: (A) ^{1}H NMR (top) and 1D CPMG (bottom) spectra, and (B) expansions of Q-OCCAHSQC spectrum. The assignments of the integrated peaks are shown (see Table 3). The ^{1}H NMR spectrum was measured using 90° excitation pulse, and the repetition time (acquisition time + relaxation delay) was set to 7.2 s corresponding to five times the longest T_{1H} of the sample (anomeric proton H-1 of α-glucose) determined with the inversion-recovery experiment. The transmitter frequency for proton was 4.7 ppm, and the spectrum width was set to 12 ppm. A low power presaturation (γB_2 = 20 Hz) was applied during the relaxation delay on water resonance. Sixteen dummy scans were used prior to acquisition. The same parameters were used for the 1D CPMG experiment. The CPMG pulse train duration for macromolecule signal suppression was set to 200 ms; τ delay was 200 μs. The Q-OCCAHSQC spectrum was measured using 8 scans per Δ-value, resulting in total of 32 scans per increment. The number of dummy scans was 32. The spectral widths in the proton and carbon dimensions were 10 ppm and 200 ppm, respectively. The transmitter frequencies for proton and carbon were 4.7 ppm and 100 ppm. A low power presaturation (γB_2 = 20 Hz) was applied during the relaxation delay on water resonance. The repetition time was set to 7.2 s. The 2D spectrum was acquired with 2.5k * 400 points. Total measurement time was 26 h 41 min. Line broadening (LB) of 1 Hz was used in apodization of ^{1}H NMR and 1D CPMG spectra. The Q-OCCAHSQC spectrum was processed with squared cosine apodization on both dimensions. The number of real points after Fourier transforms of the ^{1}H NMR, 1D CPMG, and Q-OCCAHSQC spectra were 32k, 32k, and 8k * 2k, respectively.

Table 1
Peak integral variation in 1D Q-OCCAHSQC experiments from methanol sample with varied carbon carrier frequency offsets. The carrier frequency offset step was 1 kHz. The integral was calibrated to 1.0 for the peak with carbon carrier frequency on-resonance.

	Offset range			
	±10 kHz	±15 kHz	±20 kHz	±25 kHz
Average	0.998	0.997	0.984	0.962
SD %	2.9%	3.4%	5.9%	8.3%
Max. error %	5.9%	−7.2%	−22.8%	−38.0%

edited approaches [53,54], and by that alleviate quantitative studies of low molecular weight metabolites. The high molecular weight components can be evaluated with use of spectral deconvolution and principal component analysis. However, it has been of some concern that the complexity of ^{1}H NMR spectra can lead errors in interpretation of the data [55,56]. Nicholson and co-workers [57] have presented an analysis of human blood plasma using a high magnetic field NMR spectrometer in concert with 2D NMR experiments, and they demonstrated the wealth of information what can be extracted with proton-carbon correlation experiments due to the good resolution of cross peaks in two dimensions. The same ideology could be used in quantitative analysis; the accuracy of quantification can be improved by employing a quantitative 2D proton-carbon correlation experiment to resolve the overlapping peaks.

As a general example of Q-OCCAHSQC in mixture analysis, a human blood plasma sample of a healthy volunteer was measured with Q-OCCAHSQC, and the spectrum was compared to ^{1}H NMR and 1D CPMG spectra. As shown in Fig. 5A, the high molecular weight part of the plasma sample gives very broad lines in the

Table 2
Cross peak integration results from the Q-OCCAHSQC spectra of strychnine sample measured with two ^{13}C carrier frequencies. The integral of the cross peak 4 with smallest ^{13}C offset (^{13}C carrier on 100 ppm) was used as the reference and calibrated to 1.0. Cross-peak integral of 17a,b was divided by two. Integrals are averages of separate experiments, standard deviation of each integration result was under 3% ($n = 3$). For assignment numbering see Ref. [6].

Assignment	^{13}C carrier on 100 ppm		^{13}C carrier on 200 ppm	
	^{13}C offset [Hz]	Normalized Integral	^{13}C offset [Hz]	Normalized Integral
15b	−9200	1.05	−21775	0.82
15a	−9200	1.01	−21775	0.80
14	−8594	1.07	−21169	0.91
11b	−7229	1.09	−19804	1.04
11a	−7229	1.07	−19804	1.03
17a,b	−7186	0.89	−19761	0.80
13	−6512	0.99	−19087	0.90
18b	−6246	0.83	−18821	0.76
18a	−6246	0.94	−18821	0.88
20b	−5970	1.01	−18545	0.92
20a	−5970	0.96	−18545	0.89
8	−5032	1.01	−17607	0.98
16	−5015	0.96	−17590	0.92
23b	−4463	1.00	−17038	0.97
23a	−4463	0.94	−17038	0.95
12	−2823	0.97	−15397	1.05
4	2066	1.00	−10509	1.01
1	2793	0.86	−9782	0.83
2	3041	0.89	−9534	0.84
22	3444	0.84	−9131	0.78
3	3577	0.97	−8997	0.92
SD %		7.3%		8.8%
Avg		0.97		0.90
Max. error %		−17.4%		−24.4%

^{1}H NMR spectrum. These signals can be attenuated by the 1D CPMG experiment. The peaks from the low molecular weight compounds are retained, and their integration is then easier. The selected peaks of α-glucose, β-glucose, alanine, lactate, and valine (Fig. 5A) were deconvoluted, and the integral of anomeric proton H1 of α-glucose was set as the reference by calibrating the value to 1.0. Similarly, the selected cross peaks of these chemicals (Fig. 5B) were integrated, and the integral of anomeric proton H1 of α-glucose was set as the reference. The relative amounts of the metabolites determined with two different NMR experiments are shown in Table 3; the average of the viable cross-peak integrals (see Fig. 5B) was used in the Q-OCCAHSQC quantification. As can be seen, the Q-OCCAHSQC results agree quite well with the 1D CPMG results. On closer examination the Q-OCCAHSQC quantification shows slightly larger proportion to all metabolites. The reason for this can be that when the signals of the high molecular weight components are attenuated during a long T_2-filtering period (200 ms) in the 1D CPMG spectrum, the intensities of the low molecular weight compounds are also affected. Naturally, T_2-attenuation occurs in some degree in the proposed Q-OCCAHSQC as the magnetization spends several milliseconds in transverse plane during the fixed periods of the pulse sequence (i.e. the CPMG-INEPT periods). The attenuation is most prominent with macromolecule resonances while resonances of the small metabolites are virtually unchanged due to their long proton T_2-values. The optimization of the CPMG-INEPT steps with respect to the Hartmann–Hahn transfer efficiency and T_2 relaxation during the XY-16 pulsing [58] may yield a more precise understanding of the magnetization transfer, and offer more accurate 2D quantification. As demonstrated by Furrer et al. [58] the ratio of 2τ and pulse width has significant effect to the Hartmann-Hahn transfer efficiency. While they changed the ratio by adjusting the inter-pulse delay, adjustment of proton pulse duration without compromising the bandwidth and tilt angle could be an additional approach worthwhile to investigate. Some of the broadband pulses like BIP [59] and power-BIBOP [60] have demonstrated a good offset tolerance with varied pulse lengths, and may be useful in this respect. The influence of T_2 relaxation in HSQC quantification has also been studied by Zhang and Gellerstedt [61]. They proposed an approach where cross peaks with the same T_2 relaxation profiles were analyzed as individual groups, so that the T_2 errors in quantification could be minimized. Therefore, it is relatively safe to perform quantification either for low molecular weight or high molecular weight components. However, comparisons between metabolites and macromolecules are not advisable due to differences between proton T_2-values of these two compound groups.

Table 3
Relative amounts of selected metabolites in human blood plasma sample. The peaks that were used in quantification are marked in Fig. 5. 1D CPMG results were extracted from the spectrum using deconvolution. Standard deviation is shown on those Q-OCCAHSQC results where more than one viable cross peak was used in quantification.

Metabolite	Relative quantity	
	1D CPMG	Q-OCCAHSQC
α-Glucose	1.00	0.99 ± 0.10
β-Glucose	1.17	1.29 ± 0.10
Alanine	0.25	0.32
Lactate	0.66	0.72
Valine	0.14	0.18 ± 0.03

The total acquisition time of the Q-OCCAHSQC experiment was relatively long, meaning that the quantification approach demonstrated above is not suitable for high-throughput analyses. The total acquisition time could be minimized by following the approach presented by Lewis and co-workers [62]. Their fast metabolite quantification, or FMQ method, applied short repetition times and truncated spectral width in the indirect ^{13}C dimension. The aromatic region was aliased in the spectrum, offering a reasonable resolution in the indirect dimension with low number of increments. Short repetition time caused partial saturation of the magnetization, but when the T_{1H} times of the analytes were close to each other, the quantitativity was still reasonable. The FMQ approach facilitated acquisition of quantitative 2D NMR spectrum within 12 min with error of 2.7% [62]. If the FMQ approach is

applied to the Q-OCCAHSQC experiment, the J_{CH} and ^{13}C offset dependence of the cross peak intensity would also be minimized, thus offering an accurate and relatively rapid quantification method for large sample sets.

5. Conclusions

The presented offset-compensated 2D proton-carbon correlated NMR experiment, Q-OCCAHSQC, offers possibility to acquire quantitative information directly from 2D integrals without need for post-processing of the integration values with ^{13}C offset-dependent correction coefficients. The proposed experiment would be useful in analysis of biomedical samples for e.g. metabonomic studies, and rapid quantification of large sample sets would be possible by employing the FMQ method. Furthermore, the experiment is applicable in normal structural elucidation, as the methyl, methylene, and methine cross peaks and the total number of non-exchanging protons could be distinguished on the basis of the cross peak integrals in the same manner as with normal ^1H NMR.

References

[1] G.F. Pauli, B.U. Jaki, D.C. Lankin, Quantitative ^1H NMR: development and potential of a method for natural products analysis, J. Nat. Prod. 68 (2005) 133–149.
[2] N.J. Serkova, C.U. Niemann, Pattern recognition and biomarker validation using quantitative^1H-NMR-based metabolomics, Expert Rev. Mol. Diagn. 6 (2006) 717–731.
[3] H. Koskela, Quantitative 2D NMR studies, Ann. Rep. NMR Spectrosc. 66 (2009) 1–31.
[4] S. Heikkinen, M.M. Toikka, P.T. Karhunen, I. Kilpeläinen, Quantitative 2D HSQC (Q-HSQC) via suppression of *J*-dependence of polarization transfer in NMR spectroscopy: application to wood lignin, J. Am. Chem. Soc. 125 (2003) 4362–4367.
[5] G.A. Morris, R. Freeman, Enhancement of nuclear magnetic resonance signals by polarization transfer, J. Am. Chem. Soc. 101 (1979) 760–762.
[6] H. Koskela, I. Kilpeläinen, S. Heikkinen, Some aspects of quantitative 2D NMR, J. Magn. Reson. 174 (2005) 237–244.
[7] H.Y. Carr, E.M. Purcell, Effects of diffusion on free precession in nuclear magnetic resonance experiments, Phys. Rev. 94 (1954) 630–638.
[8] S. Meiboom, D. Gill, Modified spin-echo method for measuring nuclear relaxation times, Rev. Sci. Instrum. 29 (1958) 688–691.
[9] D.J. Peterson, N.M. Loening, QQ-HSQC: a quick, quantitative heteronuclear correlation experiment for NMR spectroscopy, Magn. Reson. Chem. 45 (2007) 937–941.
[10] N.M. Loening, J. Keeler, G.A. Morris, One-dimensional DOSY, J. Magn. Reson. 153 (2001) 103–112.
[11] L. Frydman, T. Scherf, A. Lupulescu, The acquisition of multidimensional NMR spectra within a single scan, Proc. Natl. Acad. Sci. USA 99 (2002) 15858–15862.
[12] N.M. Loening, M.J. Thrippleton, J. Keeler, R.G. Griffin, Single-scan longitudinal relaxation measurements in high-resolution NMR spectroscopy, J. Magn. Reson. 164 (2003) 321–328.
[13] M.H. Levitt, Composite pulses, Prog. Nucl. Magn. Reson. Spectrosc. 18 (1986) 61–122.
[14] M.H. Levitt, Composite pulses, in: D.M. Grant, R.K. Harris (Eds.), Encyclopedia of Nuclear Magnetic Resonance, Wiley, New York, 1996, pp. 1396–1411.
[15] M.H. Levitt, R. Freeman, NMR population inversion using a composite pulse, J. Magn. Reson. 33 (1979) 473–476.
[16] M.H. Levitt, Symmetrical composite pulse sequences for NMR population inversion. I. Compensation of radiofrequency field inhomogeneity, J. Magn. Reson. 48 (1982) 234–264.
[17] D.J. Lurie, Numerical design of composite radiofrequency pulses, J. Magn. Reson. 70 (1986) 11–20.
[18] M.H. Levitt, R. Freeman, Compensation for pulse imperfections in NMR spin-echo experiments, J. Magn. Reson. 43 (1981) 65–80.
[19] H.P. Hetherington, D.L. Rothman, Phase cycling of composite refocusing pulses to eliminate dispersive refocusing magnetization, J. Magn. Reson. 65 (1985) 348–354.
[20] C.S. Poon, R.M. Henkelman, 180 refocusing pulses which are insensitive to static and radiofrequency field inhomogeneity, J. Magn. Reson. 99 (1992) 45–55.
[21] R. Tycko, H.M. Cho, E. Schneider, A. Pines, Composite pulses without phase distortion, J. Magn. Reson. 61 (1985) 90–101.
[22] R. Freeman, J. Friedrich, X.-L. Wu, A pulse for all seasons. Fourier transform spectra without a phase gradient, J. Magn. Reson. 79 (1988) 561–567.
[23] M.H. Levitt, R.R. Ernst, Composite pulses constructed by a recursive expansion procedure, J. Magn. Reson. 55 (1983) 247–254.
[24] M. Garwood, L. DelaBarre, The return of the frequency sweep: designing adiabatic pulses for contemporary NMR, J. Magn. Reson. 153 (2001) 155–177.
[25] E. Kupče, Applications of adiabatic pulses in biomolecular nuclear magnetic resonance, Methods Enzymol. 338 (2002) 82–111.
[26] K. Hallenga, G.M. Lippens, A constant-time ^{13}C–^1H HSQC with uniform excitation over the complete ^{13}C chemical shift range, J. Biomol. NMR 5 (1995) 59–66.
[27] R.D. Boyer, R. Johnson, K. Krishnamurthy, Compensation of refocusing inefficiency with synchronized inversion sweep (CRISIS) in multiplicity-edited HSQC, J. Magn. Reson. 165 (2003) 253–259.
[28] E. Kupče, R. Freeman, Compensated adiabatic inversion pulses: broadband INEPT and HSQC, J. Magn. Reson. 187 (2007) 258–265.
[29] H. Hu, K. Krishnamurthy, Doubly compensated multiplicity-edited HSQC experiments utilizing broadband inversion pulses, Magn. Reson. Chem. 46 (2008) 683–689.
[30] S. Keppetipola, W. Kudlicki, B.D. Nguyen, X. Meng, K.J. Donovan, A.J. Shaka, From gene to HSQC in under five hours: high-throughput NMR proteomics, J. Am. Chem. Soc. 128 (2006) 4508–4509.
[31] S.A. Smith, T.O. Levante, B.H. Meier, R.R. Ernst, Computer simulations in magnetic resonance. An object-oriented programming approach, J. Magn. Reson. A 106 (1994) 75–105.
[32] MATLAB version 6.5.0, The MathWorks Inc., Natick, Massachusetts, 2002.
[33] T.-L. Hwang, P.C.M. van Zijl, M. Garwood, Fast broadband inversion by adiabatic pulses, J. Magn. Reson. 133 (1998) 200–203.
[34] T. Gullion, D.B. Baker, M.S. Conradi, New, compensated Carr–Purcell sequences, J. Magn. Reson. 89 (1990) 479–484.
[35] T.E. Skinner, K. Kobzar, B. Luy, M.R. Bendall, W. Bermel, N. Khaneja, S.J. Glaser, Optimal control design of constant amplitude phase-modulated pulses: application to calibration-free broadband excitation, J. Magn. Reson. 179 (2006) 241–249.
[36] R. Fu, G. Bodenhausen, Evaluation of adiabatic frequency-modulated schemes for broadband decoupling in isotropic liquids, J. Magn. Reson. A 119 (1996) 129–133.
[37] R. Laatikainen, M. Niemitz, W.J. Malaisse, M. Biesemans, R. Willem, A computational strategy for the deconvolution of NMR spectra with multiplet structures and constraints: analysis of overlapping ^{13}C–^2H multiplets of ^{13}C enriched metabolites from cell suspensions incubated in deuterated media, Magn. Reson. Med. 36 (1996) 359–365.
[38] F. Bloch, Nuclear induction, Phys. Rev. 70 (1946) 460–485.
[39] O.W. Sørensen, G.W. Eich, M.H. Levitt, G. Bodenhausen, R.R. Ernst, Product operator formalism for the description of NMR pulse experiments, Prog. Nucl. Magn. Reson. Spectrosc. 16 (1983) 163–192.
[40] R.R. Ernst, G. Bodenhausen, A. Wokaun, Principles of Nuclear Magnetic Resonance in One and Two Dimensions, Clarendon Press, Oxford, 1990 (Chapter 2).
[41] K.E. Kövér, G. Batta, K. Fehér, Accurate measurement of long-range heteronuclear coupling constants from undistorted multiplets of an enhanced CPMG-HSQMBC experiment, J. Magn. Reson. 181 (2006) 89–97.
[42] E.J. Wells, H.S. Gutowsky, NMR spin-echo trains for a coupled two-spin system, J. Chem. Phys. 43 (1965) 3414–3415.
[43] A. Allerhand, Analysis of Carr–Purcell spin-echo NMR experiments on multiple-spin systems. I. The effect of homonuclear coupling, J. Chem. Phys. 44 (1966) 1–9.
[44] R.R. Ernst, G. Bodenhausen, A. Wokaun, Principles of Nuclear Magnetic Resonance in One and Two Dimensions, Clarendon Press, Oxford, 1990. pp. 206–209.
[45] B. Luy, J.P. Marino, ^1H–31P CPMG-correlated experiments for the assignment of nucleic acids, J. Am. Chem. Soc. 123 (2001) 11306–11307.
[46] H. Koskela, I. Kilpeläinen, S. Heikkinen, LR-CAHSQC: an application of a Carr–Purcell–Meiboom–Gill-type sequence to heteronuclear multiple bond correlation spectroscopy, J. Magn. Reson. 164 (2003) 228–232.
[47] H. Koskela, I. Kilpeläinen, S. Heikkinen, CAGEBIRD: improving the GBIRD filter with a CPMG sequence, J. Magn. Reson. 170 (2004) 121–126.
[48] E. Kupče, R. Freeman, G. Wider, K. Wüthrich, Suppression of cycling sidebands using bi-level adiabatic decoupling, J. Magn. Reson. A 122 (1996) 81–84.
[49] E. Kupče, R. Freeman, Compensation for spin–spin coupling effects during adiabatic pulses, J. Magn. Reson. 127 (1997) 36–48.
[50] E. Kupče, Effect of sweep direction on sidebands in adiabatic decoupling, J. Magn. Reson. 129 (1997) 219–221.
[51] M. Ala-Korpela, ^1H NMR spectroscopy of human blood plasma, Prog. Nucl. Magn. Reson. Spectrosc. 27 (1995) 475–554.
[52] T. Kolokolova, O. Savel'ev, N. Sergeev, Metabolic analysis of human biological fluids by ^1H NMR spectroscopy, J. Anal. Chem. 63 (2008) 104–120.
[53] R.A. de Graaf, K.L. Behar, Quantitative ^1H NMR spectroscopy of blood plasma metabolites, Anal. Chem. 75 (2003) 2100–2104.
[54] L.H. Lucas, C.K. Larive, P. Stone Wilkinson, S. Huhn, Progress toward automated metabolic profiling of human serum: comparison of CPMG and gradient-filtered NMR analytical methods, J. Pharm. Biomed. Anal. 39 (2005) 156–163.
[55] M. Ala-Korpela, Critical evaluation of ^1H NMR metabonomics of serum as a methodology for disease risk assessment and diagnostics, Clin. Chem. Lab. Med. 46 (2008) 27–42.
[56] T.K. Karakacha, P.D. Wentzell, J.A. Walter, Characterization of the measurement error structure in 1D ^1H NMR data for metabolomics studies, Anal. Chim. Acta 636 (2009) 163–174.

[57] J.K. Nicholson, P.J.D. Foxall, M. Spraul, R.D. Farrant, J.C. Lindon, 750 MHz ^{1}H and ^{1}H–^{13}C NMR spectroscopy of human blood plasma, Anal. Chem. 67 (1995) 793–811.
[58] J. Furrer, F. Kramer, J.P. Marino, S.J. Glaser, B. Luy, Homonuclear Hartmann–Hahn transfer with reduced relaxation losses by use of the MOCCA-XY16 multiple pulse sequence, J. Magn. Reson. 166 (2004) 39–46.
[59] M.A. Smith, H. Hu, A.J. Shaka, Improved broadband inversion performance for NMR in liquids, J. Magn. Reson. 151 (2001) 269–283.
[60] K. Kobzar, T.E. Skinner, N. Khaneja, S.J. Glaser, B. Luy, Exploring the limits of broadband excitation and inversion. II. Rf-power optimized pulses, J. Magn. Reson. 194 (2008) 58–66.
[61] L. Zhang, G. Gellerstedt, Quantitative 2D HSQC NMR determination of polymer structures by selecting suitable internal standard references, Magn. Reson. Chem. 45 (2007) 37–45.
[62] I.A. Lewis, S.C. Schommer, B. Hodis, K.A. Robb, M. Tonelli, W.M. Westler, M.R. Sussman, J.L. Markley, Method for determining molar concentrations of metabolites in complex solutions from two-dimensional ^{1}H–^{13}C NMR spectra, Anal. Chem. 79 (2007) 9385–9390.
[63] T. Fujiwara, K. Nagayama, Composite inversion pulses with frequency switching and their application to broadband decoupling, J. Magn. Reson. 77 (1988) 53–63.